AIAA SciTech Forum
6-10 January 2020, Orlando, FL
AIAA Scitech 2020 Forum

10.2514/6.2020-0067

Development of Sorbitol-Based Solid Rocket Motors for Propulsion Education

Kylar Moody*, Andrew Walsh†, Alvin Ngo‡, Seabrook Whyte§, Austin Stottlemyre¶, Kurt Rouser‖
Oklahoma State University, Stillwater, OK, 74078-5016

The purpose of this study was to design and fabricate potassium-nitrate/sorbitol (KNSB) solid rocket motors, and quantify the performance for use in an undergraduate laboratory. Commercially available solid rocket motors exhibit high performance and reliability; though they are expensive and pose safety concerns and difficulties for teaching purposes. Thus, there is a critical need to establish a manufacturing process for a low-cost, high-reliability propellant that is safe to incorporate into an undergraduate aerospace propulsion laboratory exercise. The KNSB rocket grains will be cast using a tubular core in a custom casting rig and fired on a custom static thrust stand. The thrust stand is outfitted with instrumentation to determine chamber pressure and thrust for use in the undergraduate laboratory. Processes for tabulating quantities such as total impulse, specific impulse, characteristic velocity, and others will be developed and evaluated for use in the laboratory. These measured quantities will be compare to modeled quantities from chemistry analysis and simulation software; this comparison of theoretical and analytical data will constitute a laboratory exercise. The use of KNSB solid rocket motors allow for affordable propellants produced utilizing simple manufacturing techniques with low energy propellants, making educational opportunities more attainable. A procedure for mixing and casting, as well as a procedure for testing and analysis will be refined for use by the students and graduate teaching assistants. The students will learn how to characterize rocket motor burn profiles and compare it to theoretical estimates, both quantitatively and qualitatively; these skills can be applied to the engineering design process in industry, academia, or government workplaces.

Nomenclature

A_b	=	Grain burning area
A_t	=	Cross-sectional area of nozzle throat
a	=	Burn rate coefficient
C_f	=	Thrust Coefficient
C^*	=	Characteristic exhaust velocity
c_p	=	Isobaric specific heat
c_v	=	Isochoric specific heat
d	=	Propellant grain inner diameter
dt	=	Time step
F	=	Thrust produced by motor
F_{avg}	=	Average thrust of motor
g	=	Gravity constant
h	=	Height
I_{sp}	=	Specific impulse
I_{total}	=	Total impulse
K_n	=	Klemmung

*Research Assistant, Mechanical & Aerospace Engineering, 201 General Academics Building, Student Member
†Research Assistant, Mechanical & Aerospace Engineering, 201 General Academics Building, Student Member
‡Research Assistant, Mechanical & Aerospace Engineering, 201 General Academics Building, Student Member
§Research Assistant, Mechanical & Aerospace Engineering, 201 General Academics Building, Student Member
¶Research Assistant, Mechanical & Aerospace Engineering, 201 General Academics Building, Student Member
‖Assistant Professor, Mechanical & Aerospace Engineering 201 General Academic Building, Associate Fellow

k_{mix} = Specific heat ratio of the mixture
L = Total grain length
m_p = Mass of propellant
n = Pressure exponent
n_i = Number of moles, products and reactants
P_c = Chamber pressure of motor
P_e = Exit gas pressure
R = Gas constant
r_b = Burn rate
r_i = Inner radius of motor casing
r_o = Outer radius of motor casing
T_{amb} = Ambient temperature
T_f = Adiabatic flame temperature
t_b = Burn time of propellant
W_p = Weight of propellant
w = Propellant grain web thickness
Δt = Time step
ΔH_f = Enthalpy of formation
ρ_p = Density of propellant
σ_R = Resultant casing stress
σ_{t_c} = Tangential stress in casing
σ_{r_c} = Radial stress in casing
Φ = Equivalence ratio

I. Introduction

As the commercialization of space becomes more prominent, there is an increase in interest for a career in space propulsion. Currently, a large portion of space propulsion centers around high-powered rocketry which can be too expensive for academic use. Thus, there is a critical need for a safe, affordable, and reliable method of instilling knowledge of rocketry within the undergraduate community pursuing careers in space propulsion. Knowledge of design, fabrication, and experimental testing of solid rocket motors (SRM) is a fundamental stepping stone for a career in space propulsion; similar procedures for developing experimental motors have been used by the amateur rocketry community. A few examples of these low cost, homemade amateur rocketry propellants include ammonium perchlorate composite (APCP) and potassium nitrite/sorbitol (KNSB) as shown in Fig. 1. KNSB is the focus of this study because sorbitol is readily available, inert, and has a lower decomposition temperature when compared to APCP motors. This makes grain manufacturing much easier, safer, and more affordable as lower temperatures pose lower threats of combustion.

Fig. 1 Example of a potassium-nitrate and sorbitol SRM static fire [1].

The goal of this study is to design, fabricate, and evaluate a sorbitol-based rocket that is safe and reliable for an undergraduate aerospace propulsion laboratory exercise. The evaluation of the KNSB SRMs will revolve around their geometric dimensions as well as thrust and chamber pressure measurements taken from a custom static fire test stand. Several derived figures of merit coming from these measurements, such as I_{sp} and C^*, are used to characterize the designed SRM.

The following objectives are designed to work towards meeting the proposed goal:

1) Evaluate the feasibility of a sorbitol-based solid rocket motor for use in an undergraduate laboratory.

2) Develop procedure to effectively manufacture and analyze sorbitol-based solid rocket motors.
3) Evaluate effectiveness of undergraduate propulsion education laboratory exercise via student responses.

Objectives 1 and 2 will involve the majority of the designing and fabricating of KNSB SRMs along with the confirmation of their manufacturing procedures. This will include the physical design and fabrication of the sorbitol-based SRM, including the manufacturing of the motor casing and mixing/casting of the propellant. This will also encompass inspection of the propellant through density ratios and destructive testing, casing strength validation, preliminary thrust stand testing, and the acquisition of necessary data such as thrust and chamber pressure. The experimental data will also necessitate validation through comparison with common SRM analysis programs, such as MotorSim and OpenRocket. Objective 3 will require implementation of the undergraduate laboratory into the Aerospace Propulsion and Power curriculum followed by collection of student responses toward the exercise.

II. Background and Theory

A. Undergraduate Aerospace Propulsion Education

The undergraduate laboratory will accompany the MAE 4243 course, Aerospace Propulsion and Power, or other courses like it. The course focuses on propulsion engines which utilize a gas as the working fluid. There is detailed design and analysis of aircraft engine cycles, such as the Brayton cycle and all variants like the turbofan, turboprop, and turbojet. Gas turbine engine cycle analysis is also discussed in detail for both on-design and off-design mission considerations. With the interest in commercial space growing, the course has also been adapted to include a multi-part lesson to overview different types of space propulsion and power systems and their fundamental concepts. The space propulsion and power section of the course could be advanced with the addition of a laboratory exercise, which builds on the fundamentals learned in the classroom and reinforces them with an out-of-class exercise. The laboratory would allow students to calculate derived quantities like total impulse, specific impulse, burn time, characteristic velocity, and burn rate based on measured quantities, like chamber pressure and thrust, to characterize the SRM and estimate its performance on a vehicle. Commercial rocket motors are too costly, as the course budget generally does not allow for such a large sum of money to be spent on activities that make up such a small portion of the course content, thus there is a need to develop affordable, reliable, and ultimately safe SRMs for this purpose. This course generally comes the semester before the students' final semester, in which they decide upon a senior design project, or capstone. This capstone generally focuses on one area in particular, which has recently grown to include rockets. With interest in commercial space rising, Oklahoma State sees the addition of this laboratory as a crucial part of the decision making process for the next generation of engineers.

B. Solid Rocket Motors

A solid rocket motor (SRM) is a rocket propulsion system that uses a solid fuel (combustible compound) and oxidizer (oxidizing compound) to generate thrust. SRMs utilize a strong exothermic reaction to convert chemical potential energy to fluid kinetic energy. Momentum is generated via an integrated nozzle and mounting pressure in its combustion chamber. High pressure fluid expands supersonically through the converging-diverging nozzle to generate thrust in the opposite direction to the momentum flux.

There are several different types of space propulsion systems used in industry today. Liquid rockets and SRMs are generally used across most of the commercial space industry, as well as hybrid solid-liquid rockets. Due to the immense complexity and general need for cryogenic cooling with liquid rockets, a SRM was chosen for use in developing the undergraduate propulsion laboratory. SRMs have been manufactured by hobbyists for many years as a cheap and safe alternative to mixing composite propellants at home. Sugars, such as sorbitol, dextrose, and sucrose, have been very appealing for their availability, cost, and stability at high temperature.

C. Potassium Nitrate Sorbitol (KNSB)

Several considerations were made when choosing the desired propellant chemistry. One of these considerations was the use of sorbitol as opposed to other sugar substitutes. Sorbitol's physical properties such as low viscosity, resistance to decomposition, and low melting point make it ideal over sucrose and dextrose [2]. A common oxidizer used among SRM hobbyists is potassium-nitrate. This is an inert, moderately reactive oxidizer, which has a moderate-high molecular weight; high molecular weight is beneficial for specific impulse.

Mixture ratio is one of the very important elements driving the performance of the SRM. The SRM can operate at a wide range of Fuel-Oxidizer Ratio (FOR), however there is a maximum value for specific impulse at some unique FOR. Several motor simulation software suggest a FOR for optimum specific impulse is 35:65 by mass. This means that 35% mass of the SRM will be sorbitol ($C_6H_{14}O_6$) and 65% mass will be potassium-nitrate (KNO_3). This result will be evaluated across a range of different FOR. When determining a FOR, a few criterion will be set. The lowest FOR to be tested is that associated with stoichiometric combustion. This is done such that the limiting reactant is the oxidizer, potassium-nitrate, and the fuel utilization is maximum. Effectively, this means all of the potassium-nitrate will be reacted, leaving only inert fuel to be rejected into the atmosphere. Applying the appropriate molar fraction to the mixture ratios will effectively determine the equivalence ratio, Φ, or the ratio of actual FOR to stoichiometric FOR on a molar basis. The combustion equation for stoichiometric equilibrium is shown below:

$$C_6H_{14}O_6 + 3.345(KNO_3) = 1.870(CO_2) + 2.490(CO) + 4.828(H_2O) + 2.145(H_2) + 1.672(N_2) + 1.644(K_2CO_3) + 0.057(KOH) \quad (1)$$

The mass fraction vs. equivalence ratio can be shown in the table below, as well as their simulated specific impulse values. The specific impulse results for KNSB SRMs will be taken from Richard Nakka's experimental data, where he varied only the FOR and held constant grain and casing geometry [3]. As we see, Nakka's results align with the simulation software. The Rocket Propulsion Elements textbook states that many rockets run fuel rich, or at a high equivalence ratio to increase the specific impulse [4]. This practice is common for both solid and liquid rockets.

Table 1 % Fuel vs I_{sp} for KNSB propellant.

% Fuel ($\frac{g}{g}$)	FOR ($\frac{g}{g}$)	Equivalence Ratio	I_{sp} (s)
25.75	0.19	1.00	161
30	0.24	1.24	163
35	0.30	1.56	164
40	0.37	1.93	160

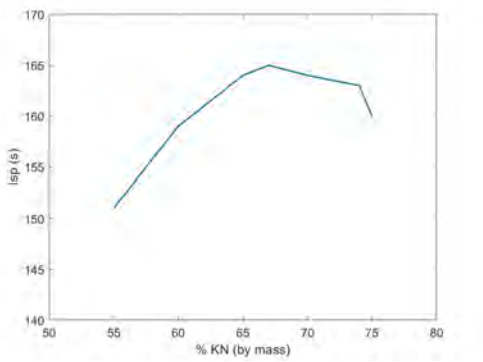

Fig. 2 Relationship between I_{sp} and % mass Potassium Nitrate in KNSB[5].

Richard Nakka has provided theory and reasoning for the composition of a KNSB based rocket propellant. It is common practice for "sugar motors" to contain 65% oxidizer by weight, potassium nitrate, and 35% fuel by weight, sorbitol. The reasoning for choosing sorbitol based motors over a conventional sucrose based motor is that the sorbitol molecule has a smaller structure when compared to a sucrose molecule. This smaller structure defines a lower melting point and therefore a larger change between the melting point and the decomposition temperature, or the temperature where the molecule breaks down. The reasoning for this mixture ratio is that it provides an optimal balance of propellant performance and physical characteristics. Increasing the percentage of oxidizer will provide enhanced performance characteristics at the cost of mixture consistency, causing increased difficulty to manufacturing processes of grains. Increasing fuel percentage will lower performance characteristics at the gain of ease of manufacturing [2].

D. Derived Figures of Merit

When static firing motors, it is possible to directly measure thrust and chamber pressure. These are important values for characterizing a motors performance, but they do not allow for easy comparison between different sizes or formulations of motors. Instead, an array of normalized figures of merit are used to accomplish these comparisons. Eqs. 2 and 3 demonstrate the calculation of total impulse (I_{total}) and specific impulse (I_{sp}). Total impulse is the total amount of force produced by a motor over its burn time. Specific impulse is simply total impulse normalized to the mass of propellant used [3]. The ideal value for KNSB I_{sp} is 164s [5].

$$I_{total} = \int_0^{t_b} F dt \tag{2}$$

$$I_{sp} = \frac{I_{total}}{W_p} \tag{3}$$

Eq. 4 shows the calculation used for thrust coefficient (C_f). This value is directly correlated to nozzle geometry. It is representative of how much the motors thrust is effected by expansion of gas through the nozzle. A simple hole with no divergent section would correlate to a thrust coefficient of 1, while a well designed nozzle for a sugar based rocket would produce a value around 1.6 [6].

$$C_f = \frac{F}{A_t P_c} \tag{4}$$

Eq. 5 is used to calculate the characteristic exhaust velocity of the propellant (C^*). This is used as a method for quantifying the combustion efficiency of a given propellant independently of nozzle performance[7][6].

$$C^* = \frac{A_t}{m_p} \int_0^{t_b} P_c dt \tag{5}$$

III. Theoretical Performance

In order to estimate some basic performance parameters, an analytical study was performed. The parameter of interest was the characteristic velocity, which allows propellants to be compared independently of the nozzle or grain geometry. In order to solve the characteristic velocity, several intermediate steps were required such as calculation of the propellant heating value, h_{PR}, the adiabatic flame temperature, T_f, and the isobaric heating value, c_p. Due to the strong dependence of c_p and temperature, an iterative methodology was utilized. The starting point for temperature was selected to be 500K, and iterated upon in a standard fashion, utilizing the tabulated temperature to determine new values of c_p. The propellant heating value, h_{PR}, is simply the difference in formation enthalpies between the reactants and products relative to the mass of reactants, which can be shown in Eq. (6). In the equation, ΔH_f is the heat of formation on a molar basis, n is the number of moles of each compound, and the subscript r or p indicates products or reactants. The sign of the tabulated value determines whether the reaction is endothermic or exothermic. For rocket applications, strong exothermic reactions are desirable thus the expected sign should be negative. It is common practice to write fuel heating value with a positive sign, as it is generally viewed in heat transfer calculations as adding heat the surroundings.

$$h_{PR} = -\frac{\sum n_i \Delta H_{f\,iP} - \sum n_i \Delta H_{f\,iR}}{m_R} \tag{6}$$

Next, the isobaric heat capacity, c_p, was calculated. This can be shown in Eq. (7), where the value for c_p can be that of the reacted mixture, gas, or multi-phase mixture. This is due to the formation of aqueous potassium-carbonate in the combustion process. The c_p value needed for the calculation of the adiabatic flame temperature, T_f, is that of the mixture including the aqueous potassium-carbonate. The equation for T_f can be shown in Eq. (8). Once this temperature is obtained, new c_p values should be obtained and iterated upon until convergence criteria on T_f are met. The values for h_{PR}, c_p, and T_f after 2 iterations did not change significantly, thus were deemed acceptable for preliminary calculations of performance. They can be shown in Table 2 at the end of this section.

$$c_p = \frac{\sum n_i c_{p\,iP}}{n_P} \tag{7}$$

$$T_f = \frac{h_{PR}}{c_p} + T_{amb} \tag{8}$$

Lastly, for a final comparison the theoretical maximum characteristic velocity, $C*$, was calculated for the propellant chemistry discussed above. The equation for characteristic velocity can be shown below in Eq. (9), where R is the specific gas constant, T_f is the adiabatic flame temperature, and k_{mix} is the mixture (including aqueous formation) ratio of specific heats. When computing the specific value of the gas constant, Nakka [5] explains that the mean molecular mass of the gaseous formations should be used in place of the mixture mean molecular mass. This is due to the fact that

only the gaseous formations behave as a gas. The mean molecular mass of the gas can be tabulated simply as the total mass divided by the number of moles of gaseous formations. Utilizing Mayer's relation for isochoric specific heat, as shown in Eq. (10), can be tabulated for any value of c_p. The isochoric specific heat, c_v, can then be used in Eq. (11) to calculate the mixture specific heat ratio. The value of k_{mix} can vary significantly as a function of temperature, thus it is important to re-tabulate the specific heats for each temperature in the iteration.

$$C^* = \sqrt{\frac{RT_f}{k_{mix}}\left(\frac{k_{mix}+1}{2}\right)^{\frac{k_{mix}+1}{k_{mix}-1}}} \tag{9}$$

$$c_p = c_v + R \tag{10}$$

$$k_{mix} = \frac{c_p}{c_v} \tag{11}$$

The table of values for the propellant theoretical performance can be shown in Table 2. The values for mean molecular mass, c_p, c_v, and k_{mix} were tabulated intermediately and can be shown in the Appendix A.

Table 2 Performance parameters calculated from chemistry.

Parameter	Value	Units
h_{PR}	2.082	$\frac{MJ}{kg}$
T_f	1455	K
C^*	2829	$\frac{ft}{s}$

With all the parameters necessary to calculate specific impulse, I_{sp}, a specific impulse vs. chamber pressure curve was generated in Matlab, as shown in Fig. 3. The equation for specific impulse can be shown in Eq. (12), where P_e is the atmospheric pressure, and P_c is the chamber pressure. Chamber pressure was simulated between 0 and 1000 psia with I_{sp} varying between 0 and 167 s^{-1}, respectively. These results will be compared to the simulated results using MotorSim as well as the reduced data from the experimental; these can be shown in the later sections.

$$I_{sp} = \frac{1}{g}\sqrt{\frac{2k_{mix}}{k_{mix}-1}\frac{RT_f}{M}\left(1-\frac{P_e}{P_c}^{\frac{k_{mix}-1}{k_{mix}}}\right)} \tag{12}$$

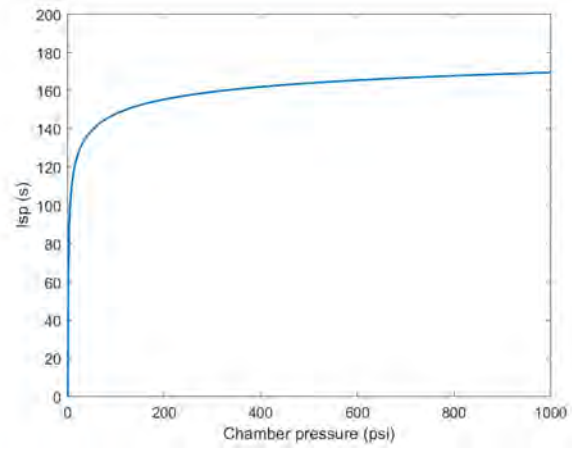

Fig. 3 Graph showing how Isp for KNSB propellant varies with chamber pressure.

IV. Simulated Performance

In addition to several comparison points based on underlying theory, a simulated motor burn was desired for grain burn performance. MotorSim, a closed source simulated motor burn software, was used for this simulation. MotorSim has the benefit of being free of charge, pre-loaded with several grain compositions, and compatible with OpenRocket, a rocket launch simulation software. MotorSim has a friendly user interface, accepts well defined parameters such as inner diameter and length of the grain, and outputs plots for burn time, chamber pressure, and thrust. Utilizing this software, a simulation of an experimental grain was created to obtain performance values for comparison. Table 3 contains several key parameters input into MotorSim. ID references the inner diameter while OD references the outer diameter. These values were defined based off of the experimental motor metal casing design and a grain to fit snugly into it.

Table 3 Key input parameters for MotorSim.

Type	Parameter	Value	Units
Casing	ID	1.38	in
Casing	OD	1.50	in
Casing	Length	3.20	in
Grain	ID	0.50	in
Grain	OD	1.33	in
Grain	Length	3.00	in

Figure 4 displays the results of overlaying the thrust and pressure curves output from the experimental grain. The simulated average thrust value, F_{avg}, is 19.5 lbf maxing out at about 21.4 lbf for maximum thrust, F_{max}. The simulated average pressure value, P_{avg}, is 167.7 psi maxing out at about 183.5 psi for maximum chamber pressure, P_{max}. The simulated burn time, t_b, is approximately 1.29 s. Derived values based on these parameters will be calculated and compared to the experimental and theoretical data in a later section. Note, the left and right side of the simulated pressure and thrust curves are illustrated as vertical lines due to constraints by the software (based off of ideal calculations).

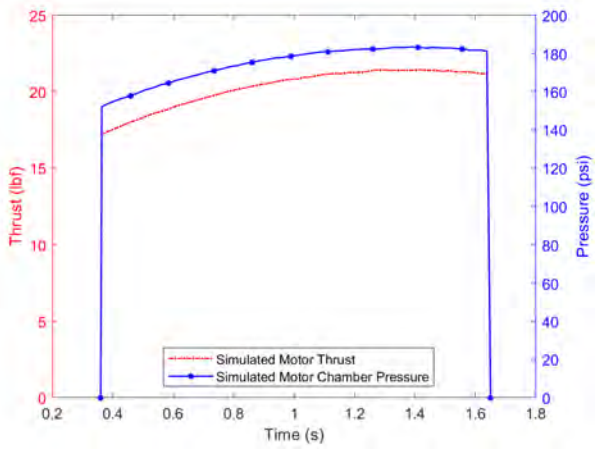

Fig. 4 Theoretical chamber pressure and thrust data obtained from MotorSim for given propellant grain dimensions.

V. Experimental Arrangements and Methodology

A. Motor Casing Development

The motor casing must be sized to withstand the chamber pressure and thermal stresses for the duration of the mission, thus some assumptions about burn profile must be made. The worst case scenario burn profile and stress location will

be used for sizing. The worst case scenario burn profile is the progressive burn profile, which is characterized by an increase in thrust and chamber pressure as time goes on. This will give the highest chamber pressure at the highest temperature, causing the highest combination of loading. The location of peak stress occurs at the inner radii of the wall and can be shown from Eqs. (13), (14), and (15). It is also important to note that for diameter to thickness ratios less than 20, the thin walled assumption is not valid. Safety is of the utmost importance when developing a lab, thus a Safety Factor (SF) of 2.5 on the yield stress of the material will be used; this will help mitigate the risk of failure. For manufacturability and cost, 6061 T6 aluminum alloy will be used in the initial casings. A COTS piece of stock was selected, in which the dimensions are listed below and the theoretical max pressure with a safety factor was tabulated. These can be shown in Table 4.

$$\sigma_{t_c} = P_c \left(\frac{r_i^2}{r_o^2 - r_i^2} \right) \left(1 + \frac{r_o^2}{r_i^2} \right) \tag{13}$$

$$\sigma_{r_c} = P_c \left(\frac{r_i^2}{r_o^2 - r_i^2} \right) \left(1 - \frac{r_o^2}{r_i^2} \right) \tag{14}$$

$$\sigma_R = \sqrt{\sigma_{r_c}^2 + \sigma_{t_c}^2} \tag{15}$$

Table 4 Casing properties and maximum pressure.

Property	Value	Units
σ_y	35000	psi
D_o	1.500	in
D_i	1.384	in
SF	2.5	-
P_{cmax}	1120	psi

The motor casing assembly will house two grains. The motor casing assembly can be shown in Fig. 5 and the list of components in Table 5. Instrumentation is not included in this list, as that will be discussed in more detail in later sections. Snap rings are used as retainers and are sized to sufficiently handle the longitudinal stresses; they allow for quick and easy changes of internals, including grains, casting tubes, and nozzles. O-Rings are used to seal the casing and keep hot gases from escaping. The nozzle used in the first phase of characterization will be a COTS nozzle, however other nozzles, such as cooled nozzles, could be used in later stages.

Table 5 Solid Rocket Motor Component List.

Component Number	Component Name
1	Snap-Ring(s)
2	O-Ring(s)
3	Nozzle
4	Plug
5	Motor Casing
6	Casting Tube
7	Grain

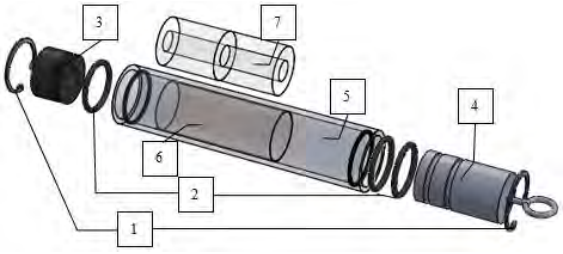

Fig. 5 Detailed view of rocket motor components.

B. Mixing and Casting of Propellant

1. Mixing

All mixing and casting for the propellant described in this paper was preformed at the College of Engineering, Architecture, and Technology Design and Manufacturing Lab. The first test conducted determined an acceptable and

repeatable mixing process. As recommended by Nakka in [8], a surfactant was added to the molten propellant mixture to lower the viscosity which made pouring it into the casing easier. In order to reduce costs, body soap was used as a cheap source of surfactant. However, this led to concern that other chemicals and water (the main ingredient of the soap) would be introduced to the mixture. In order to mitigate this, 3 different mixtures would be made. One without the surfactant, one with liquid body soap as the surfactant, and one with the water boiled out of the soap to be used as the surfactant.

First, a 65/35 by weight of potassium nitrate to sorbitol was measured out using scales. Then the potassium nitrate and the sorbitol were separately ground using a blender. They were then combined and mixed by gently turning a closed container for a predetermined amount of time, in this case around 10 minutes. This ratio and process was followed for each of the following tests to come.

All three mixtures were melted on an electric skillet (Fig. 6) and maintained at 250 degrees Fahrenheit for the duration of the cook. The mixture without the surfactant was simply melted and poured out on a cool surface where it was let to cool until it could be handled and formed into small rolls. For one of the mixtures containing the body wash for surfactant, the propellant was melted and approximately half an ounce of the body wash was added. For the final mixture, the body soap was added to the skillet before the propellant mixture and let to cook to evaporate the water out of the soap. The propellant was then added and the process continued as previously stated.

Ambient humidity was also a concern in the mixing process. In an attempt to test what effect it had the humidity at the time was noted and six rolls were made from each mixture: three immediately put in a Ziploc bag to cure so the humidity exposure was minimal and three let to cure outside of the bag.

Fig. 6 The propellant/oxidizer molten mixture.

Fig. 7 The propellant/oxidizer molten mixture.

After the propellant rolls were cured for two days, then tested for ignition. A common household grill lighter was used to light the propellant rolls as to keep hands away from the propellant when igniting. A picture of a burn can be seen in Fig. 7. It was noted that the rolls that cured outside of Ziploc bags were more difficult to light than those that cured inside Ziploc bags.

2. Casting

Le Breton and Ribéreau looked at the casting process and its impact on small solid rocket motor internal ballistics. They characterized effects of casting with and without a mandrel, with and without casting casing rotation, and with single vs. multiple pour points on ballistic performance. They found that when casting hydroxyl-terminated polybutadiene/ammonium perchlorate/aluminum (HTPB/AP/Al 14/68/18) propellant, the use of a mandrel showed higher consistency in terms of chamber pressure and burn profile. They also observed a small difference in burn rate consistency with rotational casting over stationary casting, however these results are small in magnitude and within the uncertainty range between specimens. These results are for a composite propellant and may show variance when sorbitol/potassium nitrite ($C_6H_{14}O_6/KNO_3$) propellant is used. The processes which used a mandrel showed higher consistency between specimens, thus a mandrel will be used moving forward with the casting process [9]. A picture of this setup can be seen below in Fig. 8, below.

Fig. 8 The casting tube mandrel where the propellant cures.

Fig. 9 The casting tube mandrel where the propellant cures.

The propellant was poured into a 38 mm rocket motor casing with a $\frac{1}{2}$" cylindrical coring rod placed in the middle. The cylindrical rod was chosen as it was the easiest to remove after curing and can still yield a near-neutral burn profile if certain surfaces are inhibited; this is known as the Bates grain. The ends of the motor casing were capped using 3D printed PLA end caps to keep the rod in place. Holes were put in the top cap to let excess propellant to leak out.

For casting grains without surfactant, the black PLA cap in Fig. 8 was placed at one end with tape over the holes to prevent leakage. The molten propellant mix was then poured into the casting tube without a coring rod in place. The coring rod was then shaved to a point and greased, then pushed through the middle of the propellant and out the large hole in the black cap. The orange cap was then placed at the flat end of the coring rod to align it properly in the casting tube. A picture of this setup can be seen below in Fig. 9. The casting setup was then placed in a plastic bag to seal off ambient humidity then cured for two days.

It was found that pieces of propellant were chipping off with the removal of the wooden coring rod despite the grease applied before placement. This lead to the use of an aluminum coring rod in place of the wooden one. This made removal easier and did not damage the propellant. All data shown in this paper was produced using grains cast using the aluminum coring rod.

C. Experimental Setup

The test stand will be configured nearly identical to the thrust stand described by Utley et al. shown in Fig. 10 [10]. This configuration allows for collection of thrust data during a static motor fire, but there is also a need to collect chamber pressure data. To accomplish this, a minor modification as shown in Fig. 11 will be made to allow for the collection of chamber pressure data during firing [6]. A detailed list of sensors and equipment used on the stand can be seen in Table 6. When a test is being performed, data from the sensors will be collected and processed by a custom LabVIEW virtual instrument (VI) panel constructed for the test stand.

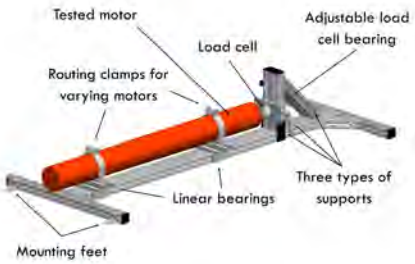

Fig. 10 Portable static fire thrust stand for solid rocket motors. Rated for 500lbs of thrust [10].

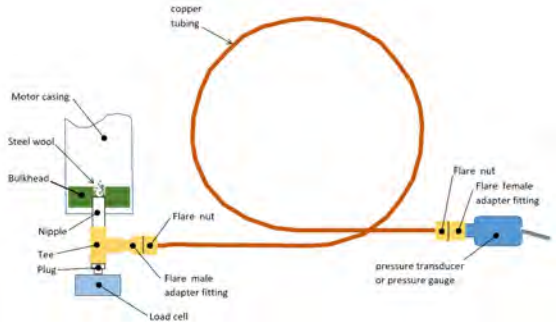

Fig. 11 Configuration for using a pressure transducer in conjunction with a load cell. The copper pipe helps dissipate heat to keep pressure transducer cool [6].

Table 6 Measurement Equipment.

Function	Manufacturer	Model
Power Supply	National Instruments	PS-15
DAQ	National Instruments	USB-6009 Multifunction Card
Load Cell	Futek	LLB400 Load Button
Voltage Amplifier	Futek	IAA100
Pressure Transducer	Omega	PX119-1.5KAI

In order to ensure the validity of the collected data, it is important to check that the readings from the sensors are calibrated properly. To accomplish this, calibration curves provided by the sensor manufacturers were used. Next a known force was applied to the load cell, and a known pressure was applied to the transducer. This was repeated for a range of values to ensure proper sensor readings. All static fire testing was performed at Unmanned Systems Research Institute (USRI) located at the Richmond Hills facility in Stillwater, Oklahoma.

D. Experimental Procedure

Prior to testing of the SRM on the portable rocket thrust stand, multiple specimen must pass the test for CATO. CATO testing can be as simple or complex as desired, sometimes equipping instrumentation to determine the cause of CATO, however for the purpose of this study, a much simpler CATO test will be performed. The rocket will be placed in a hole in the ground and ignited remotely with a car battery and long wire leads. The rocket will be positioned in the hole so that it is firing downward. If 3 specimen fire without CATO, then the following procedures will be used to conduct the static fire motor testing on the portable rocket thrust stand. If a single specimen fails CATO testing, then an additional 3 specimen will be manufactured and fired remotely in the same arrangement until all three pass with relative repeatability between specimens.

1) Secure rocket motor to test stand by means of routing clamps, move motor assembly along the bearings until the forward end of the motor is in contact with the load cell, connect instrumentation to DAQ, record date, time and ambient conditions in the lab book and DAQ, and ensure all personnel have eye and ear protection and are instructed on location and use of the nearby fire extinguisher (within 10 feet of the stand).
2) Insert electrical motor igniter (with stripped leads) into the motor until the igniter head is seated against the bulkhead and forward-most propellant grain.
3) Clear personnel within 10 feet of the rocket stand and downstream of the nozzle, begin data acquisition, and close high bay door to protect from noise, exhaust, and fire hazards.
4) Count down from 5 and begin ignition sequence using the test stand's LabVIEW VI shown in Fig. 12.
5) Disconnect wire leads from the power source and end data collection, disconnect instrumentation, allow motor to cool to touch before removing motor from stand by releasing clamps, and dispose of single-use parts.

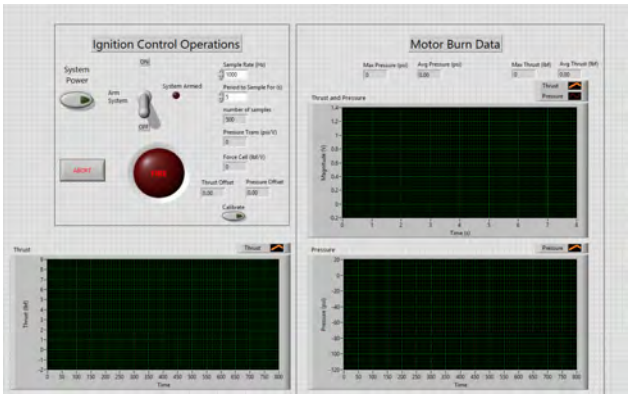

Fig. 12 Ignition control panel from thrust stand VI used to fire the motor.

VI. Results and Discussion

A. Propellant Roll Test Results

The propellant test rolls with surfactant (both cured in the sealed bag and in open air) would not burn when the lighter flame was held to them. Instead, the propellant rolls just melted as they got hot. The propellant roll that did not have surfactant but was cured in the open air yielded the same result. The propellant roll without surfactant that was cured in the sealed bag was the only propellant roll to successfully combust. The 5 g roll (approximately 2 in long) completely combusted in approximately 22 s when ignited at one end of the roll.

B. Propellant Inspection Results

After the grains have been given ample time, approximately 2 days, to cure, they can be inspected for quality. To check this quality a density calculation is necessary. To obtain density, the weight can be obtained using a scale and the volume measured using calipers. By comparing the density of the grain to the ideal density of KNSB, 1.841 $\frac{g}{cm^s}$, one can theorize the amount of imperfections, voids, or air bubbles within the grain. The target ratio of real/ideal density is between 0.99 - 0.95 as shown Table 8. This is an acceptable range that will negligibly impact performance. Anything below 0.95 will notably impact performance and could present safety hazards from the large air pockets in the grain[2].

A destructive inspection on the grain, cutting the grain to view the internal structure, is also an option for validating quality. However, the KNSB grains can be brittle and fall apart during the destructive inspection. This would make it difficult to distinguish the difference between imperfections caused from casting and damages caused by inspection.

Table 7 Density ratios of grains produced using aluminum core rod.

Grain	Ratio
1	0.974
2	0.942
3	0.977
4	0.985
5	0.971
6	0.982
7	0.956

Table 8 Ratios of actual densities to theoretical density values and acceptable ranges for quality [2].

Density Ratio	Assessment
1.00	Ideal only, not realizable in practice
0.95-0.99	Very good to excellent quality, essentially no voids or porosity
0.90-0.94	Fair to good quality, some porosity, voids, or other flaws
0.85-0.89	Low to marginal quality, significant porosity or flaws. If density ratio is low due to hidden flaws, grain should be discarded
<0.85	Serious flaws exist. Discard

C. Experimental Test Results

For the experimental portion of the analysis, a motor was test fired on the motor testing stand. The nozzle was 3D printed in nylon using selective laser sintering, while the propellant and motor casing used were made as described previously. A custom 3D printed nozzle had to be used due to the motor casing being slightly smaller than a normal commercial one. This can be shown in Figs. 13 and 14.

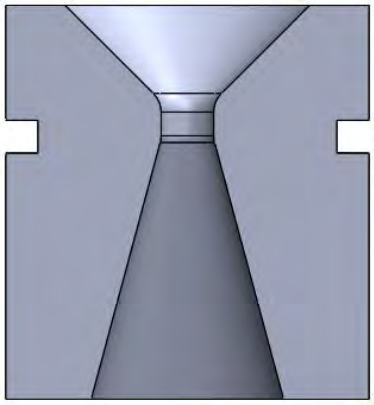

Fig. 13 Solidworks section view of nozzle used for testing.

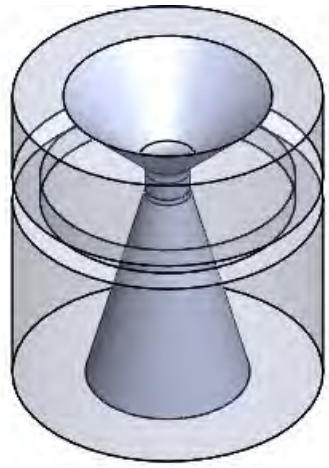

Fig. 14 Solidworks isometric view of nozzle used for testing.

The resulting thrust and chamber pressure can be seen below in Figs. 15 and 16. Something of note is that the chamber pressure increases to the MotorSim predicted value and then steadily decreases after its initial spike. This is likely a result of the 3D printed nozzle ablating causing the throat area to expand during the fire. The increase in throat area decreases exhaust velocity, but the thrust is able to remain relatively constant due to the increased mass flow rate. In future tests with a less ablative nozzle, it is expected the MotorSim and experimental results would line up better.

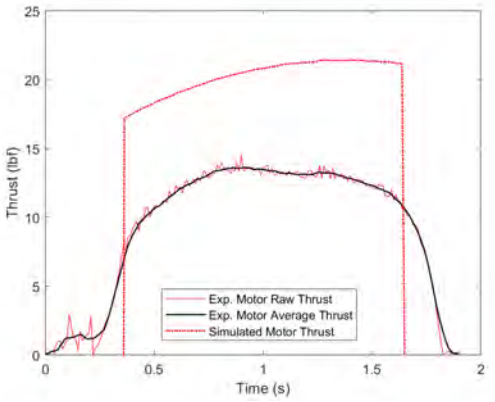

Fig. 15 Thrust data obtained from experimental and simulated motor burns.

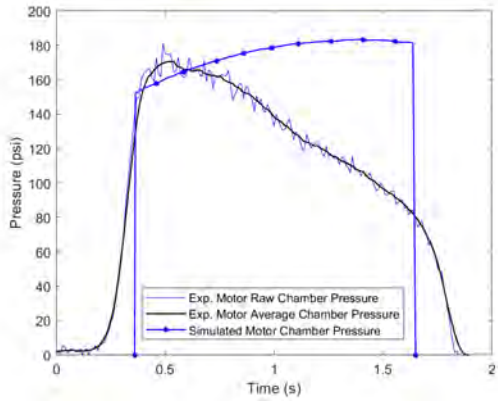

Fig. 16 Chamber pressure data obtained from experimental and simulated motor burns.

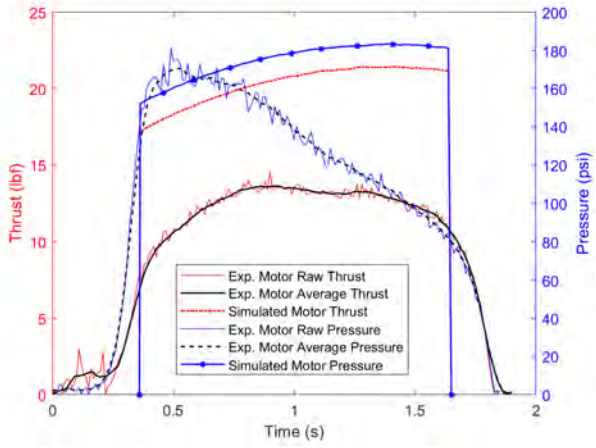

Fig. 17 Chamber pressure and thrust data from the experimental test overlayed on the simulated results.

Before derived figures of merit can be calculated, it is important to establish which portion of the data should be used for analysis. The widely accepted method is to calculate pressure and thrust values over the burn time which is defined as lasting from 75% of the max chamber pressure value until the aft tangent bisector on the thrust curve. MATLAB was used to calculate these values from the raw data.

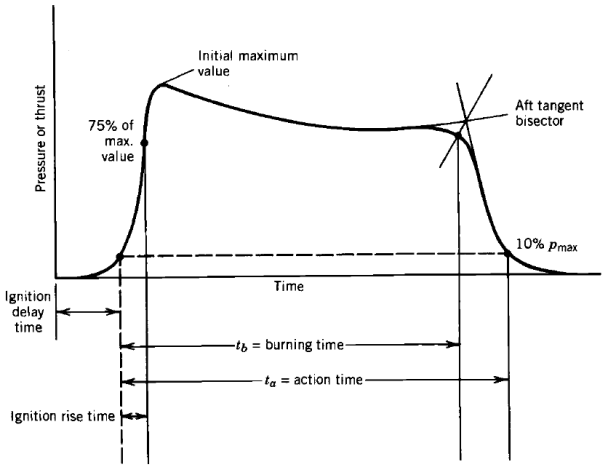

Fig. 18 An illustration of how to calculate burn time from a thrust curve graph [11].

Using the burn time value, maximum and average readings for thrust and pressure for both simulated and experimental motor tests can be calculated. I_{total} can also be calculated from this data. These values are located in Table 9.

Table 9 Performance data for tested motors.

Motor	t_b (s)	F_{max} (lbf)	F_{avg} (lbf)	P_{max} (psi)	P_{avg} (psi)	$I_{total}(s)$
Simulated	1.29	21.4	19.5	183.5	167.7	25.2
Experimental	1.32	14.7	12.3	181.3	133.7	16.25

D. Derived Results

The theoretical data is derived from the baseline chemistry from the combustion events from KNSB motors. The simulated data is from the MotorSim simulation of the cylindrical core motor burn. The experimental data is from the experiment described in the 'Experimental Arrangements and Methodology' section. Notably, the percent differences are high ($\approx 40\%$). This is mainly due to constraints from MotorSim (for the simulated data set) and an unoptimized nozzle for the experimental SRM. The derived figures of merit for the theoretical, simulated, and experimental data sets in Tables 10 and 11. Several values seem reasonable such as the thrust coefficients.

Table 10 Derived Figures of Merit for simulated motor.

FOM	Theoretical	Simulated	%Difference
$I_{sp}(s)$	164	110	39.4
C_f	1.6	1.9	17.1
$C^*(\frac{ft}{s})$	2981	1889	39.8

Table 11 Derived Figures of Merit for experimental motor.

FOM	Theoretical	Experimental	%Difference
$I_{sp}(s)$	164	71	79.1
C_f	1.6	1.5	6.5
$C^*(\frac{ft}{s})$	2981	1541	59

E. OpenRocket Simulation

In order to evaluate the functionality of the motor that was developed, a simulated flight test was performed. To accomplish this, a combination of the measured thrust curve and motor was was used to create a custom OpenRocket motor file. This motor was then placed into a model of a standard commercial off the shelf rocket kit. The results of the simulation are plotted in Fig. 20. According to the simulation, if this configuration were to actually launch the rocket would achieve an altitude of approximately 100ft.

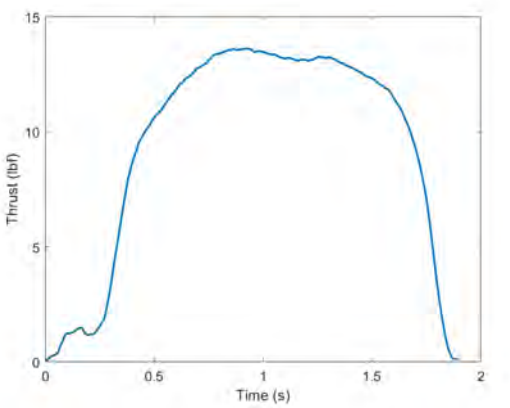

Fig. 19 Thrust curve used for open rocket simulation. This was created from a rolling average over 10 data points of the raw thrust data collected form the experimental motor.

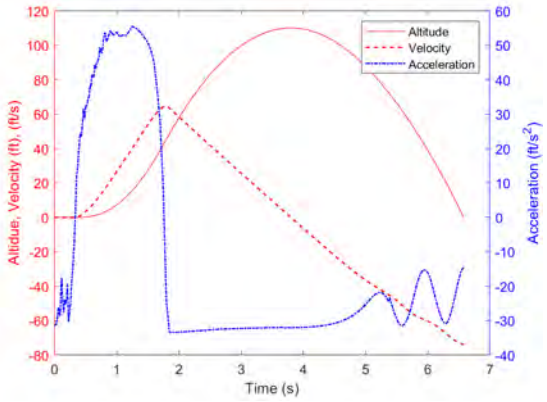

Fig. 20 Simulated rocket launch using the recorded thrust curve from the experimental motor. The rocket used in this simulation is 13.8" long, 2" diameter, and weighs 1.24lbs. At approximately 4 seconds apogee is achieved.

VII. Undergraduate Propulsion Laboratory

The main purpose of developing KNSB SRMs was to have an affordable method of repetitive motor burns allowing students to observe and experience rocket propulsion adequately. The experimental results above suggest that the development of an undergraduate propulsion laboratory is feasible. The lab will be based on several key "take-aways" that are outlined below.

1) Visualize the performance of a SRM defined by experimental performance data using MotorSim.
2) Obtain experimental data from a SRM burn.
3) Calculate and plot specific impulse of the SRM, I_{sp}, as a function of chamber pressure, P_c.
4) Calculate key derived figures of merit integral to characterizing rocket performance, such as total impulse I_total, thrust coefficient C_f, and characteristic velocity C^*.
5) Calculate exit pressure and exit Mach Number of the propellant (KNSB) given certain values; characterize exit flow as over/under expanded.
6) Compare and contrast theoretical and experimental data for the given SRM.

First the students will perform a simulated burn using software such as MotorSim to gain an idea of how the experimental data should look. Next the students will observe several SRMs being fired. After each fire, students will take thrust and chamber pressure data. For the sake of not overwhelming the undergraduate propulsion students, especially if the laboratory is meant for base level space propulsion, the KNSB motors will be mixed and cast by teaching assistants. After the fires, the students will calculate all the derived figures of merit outlined in the 'Derived Figures of Merit' section for both the theoretical case and the experimental case. These values will be compared and a percent difference will be calculated. In addition to these, the students will use compressible flow relations to describe the exit flow; these relations are a function Mach number and specific heat ratio, which are easily calculated from the experimental data.

All software and prerequisite knowledge defining the undergraduate laboratory are fundamental to current era engineering students and do not require excessive out-of-class learning. Students will exit the laboratory section with a basic understanding of rocket propulsion along with experience recording/processing motor burn data. The derived figures of merit calculations will allow students to exercise their comparing and contrasting skills. Using and learning OpenRocket will exercise baseline programming along with physical parameter interpretation from the experimental data obtained.

VIII. Summary

A. Key Findings

1. Propellant Mixing and Casting

For this project, the only propellant mixture ratio used was 65:35 potassium nitrate:sorbitol mixture. No other ratios or chemicals were used in this process. The propellant was unable to ignite when body wash was used as the surfactant. This resulted in all of the tests being run without the use of surfactant. Additionally, it was found that an aluminum coring rod was the best selection for easy removal without damaging the propellant grain.

2. Comparison of Results

Comparing the results between the theoretical calculations and the experimental data illuminated the large percent differences. This in part was due to the nozzle utilized for the SRM. The nozzle was unoptimized and thus had significantly lower chamber pressure than what was needed. The result was proper coefficient of thrust but insufficient specific impulse. To fix this, an optimized nozzle should be designed for the SRM.

3. MotorSim and OpenRocket Software

The GUI of both software are simple and intuitive. This allows for easy integration into an undergraduate laboratory procedure. They will allow students to obtain simulated data from their propellant grains prior to actually experiencing the motor fires. The simulated rocket launch would add a physical perspective invaluable for students experiencing rocket propulsion for the first time. Unfortunately, there are several constraints connected the software. MotorSim was last updated in 2011 making it slowly becoming outdated. Being closed source, the underlying equations defining the simulated thrust and pressure curves are unknown making exact comparisons difficult. A newer and up-to-date software could be a viable pathway to take in terms of simulated data.

4. Undergraduate Propulsion Laboratory

A trial laboratory exercise was developed and incorporated into the MAE 4243 course described above. The total cost of teaching the laboratory is relatively low in comparison to most other hands-on options for teaching aerospace propulsion.

B. Meeting Objectives

The design and fabrication of a sorbitol-based solid rocket motor was necessary to complete Objective 1. The feasibility of KNSB SRM was demonstrated after successful ignition of the motors during the motor safety tests (CATO), and after comparing propellant mixing and casting methods. An initial design was created in MotorSim followed by the manufacturing of the motor casing. A procedure was designed for the mixing and casting of the KNSB propellant and the propellant, in addition to density and deformity inspection prior to testing. A CATO test was performed on the inspected propellant to prepare for thrust stand testing.

Performance parameters were successfully obtained and analyzed from a KNSB SRM developed as a result of objective 1. Objective 2 was met due to the thrust and chamber pressure values obtained for each motor created, enabling analysis described in this paper as well as demonstrating manufacturability. The collected data was analyzed for various derived figures of merit. The data was then compared with MotorSim and OpenRocket results, constituting the undergraduate laboratory and enabling evaluation for objective 3. The values from Table 9 show that the experimental values are within respectable margins of other SRM.

C. Lab Results

Below is an example of a firing which was used for tabulation of results in the undergraduate laboratory. It is important to note that the overall size of the SRM has increased compared to the SRM used in prototyping and testing, which changed the performance parameters. A COTS nozzle was also used in lieu of an experimental nozzle as it is well characterized and easy to obtain. The results can be shown in Fig. 21 where average thrust and pressure are plotted as a function of time. There is a clear trend between thrust and chamber pressure, which is consistent with physics.

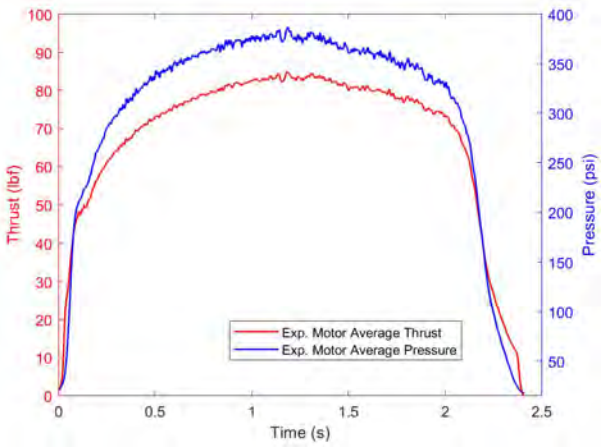

Fig. 21 Chamber pressure and thrust from data collected in lab.

Students are tasked with completion of the laboratory exercise, which includes a data reduction element. During this trial laboratory, they were also tasked with comparison of the KNSB SRM to a commercial double-base SRM using a commercial nozzle, which allows comparison of the homemade motors to a well characterized motor. Given the thrust and pressure curve shown above in Fig. 21 for the KNSB SRM, the values shown in Table 12 can be calculated. This is an example of data tabulated by a student in the MAE 4243 course given the raw thrust and pressure data as well as a few unknowns such as propellant mass, nozzle geometry, grain geometry, and ambient conditions.

Table 12 Performance data for motor tested in lab.

t_b (s)	m_{dot} (lbm/s)	F_{max} (lbf)	F_{avg} (lbf)	P_{max} (psi)	P_{avg} (psi)	$I_{total}(s)$	$I_{sp}(s)$	C_f	$C^*(ft/s)$
1.79	0.6652	85.88	78.07	392.8	354.57	139.9	117.37	1.7	2225

This laboratory exercise was incorporated into the MAE 4243 Aerospace Propulsion and Power course at Oklahoma State University as part of the educational curriculum. The laboratory exercise was given as an individual exercise which allowed collaboration between group members. At the end of the lab, the two questions below were asked to evaluate the labs effectiveness at teaching solid rocket analysis.

1) Rate the effectiveness of using the rocket lab to facilitate learning about solid rocket performance analysis.
2) Rate the effectiveness of using the rocket lab to facilitate learning about solid rocket propellant.

The class overall responded well to the lab exercise as Table 13 and 14 show the classroom feedback. The sample size was 64; the statistics for questions 1 and 2 are shown in Table 15, which give significant evidence that the students had a positive response to the laboratory exercise, meeting objective 3.

Table 13 Responses to Question 1.

Assessment	Number of responses
Not Effective	0 students (0%)
	0 students (0%)
Somewhat Effective	12 Students (19%)
	31 Student (48%)
Highly Effective	21 Students (33%)

Table 14 Responses to Question 2.

Assessment	Number of responses
Not Effective	1 students (2%)
	4 students (6%)
Somewhat Effective	16 Students (25%)
	29 Student (45%)
Highly Effective	14 Students (22%)

Table 15 Student responses to laboratory effectiveness.

Question	Average	Standard Deviation
Question 1	4.14	0.709
Question 2	3.80	0.911

D. Future Work

Expansion on this project would be done by conducting more live fire testing using COTS nozzles. This will provide optimal area ratio for higher thrust and specific impulse along with increased chamber pressure. The use of a pure surfactant or various different surfactants would be advisable. Additional surfactants to be tested should not include water or nonessential chemicals as ingredients. Utilizing pressure curing could be an addition advantage to the mixing and casting process. To improve the laboratory in the future, different burn profiles could evaluated; this would be attained by using different cores (star, double anchor, etc.) in the casting process. Also incorporating a physical rocket launch utilizing the KNSB motors could add a practical application of the SRM analyzed in the lab. Lastly, is also recommended to try using different fuel:oxidizer mixtures to see if other ratios work better than the 35/65 ratio for ignition and performance characteristics.

Acknowledgments

We would like to acknowledge Thomas Coulon and Lucas Utley for their assistance in mixing propellant and general input into developing rocket motors.We would also like to thank Lucas Utley for collecting laboratory data.

References

[1] Erik Engheim, "Why Can Sugar be Used as Rocket Fuel?" , 2017. URL https://medium.com/@Jernfrost/why-can-sugar-be-used-as-rocket-fuel-a68678677ebc, [Online; accessed April 4, 2017].

[2] Nakka, R., *KNSB Propellant*, 2018 (accessed February 3, 2018). URL www.nakka-rocketry.net/sorb.html#Theoretical.

[3] Nakka, R., *Solid Rocket Motor Theory – Impulse and C-star*, 2018 (accessed February 3, 2018). URL https://www.nakka-rocketry.net/th_imp.html.

[4] Sutton, G., and Biblarz, O., *Rocket Propulsion Elements*, 9th ed., Wiley, 2016.

[5] Nakka, R., *KN-Sorbitol Propellant Chemistry and Performance Characteristics*, 2018 (accessed February 3, 2018). URL https://www.nakka-rocketry.net/sorbchem.html.

[6] Nakka, R., *Measuring Chamber Pressure and Determining C-Star and Thrust Coefficient*, 2018 (accessed February 3, 2018). URL www.nakka-rocketry.net/sorb.html#pressure-measurement.html.

[7] Nakka, R., *Technical Notepad 3 – KNSB Ideal Performance Calculations*, 2018 (accessed February 3, 2018). URL https://www.nakka-rocketry.net/techs2.html.

[8] Nakka, R., *Curing KNSB Under Pressure*, 2018 (accessed February 3, 2018). URL https://www.nakka-rocketry.net/sorb.html.

[9] Le Breton, P., and Ribéreau, D., "Casting Process Impact on Small-Scale Solid Rocket Motor Ballistic Performance," *Journal of Propulsion and Power*, Vol. 18, No. 6, 2002, pp. 1211–1217. URL https://doi.org/10.2514/2.6055.

[10] Utley, L., Foster, G., and Rouser, K., "Design and Evaluation of a Portable, Flexible-Use Rocket Thrust Stand," , 2017. Unpublished Manuscript.

[11] Mattingly, J. D., and Ohain, H. V., *Elements of Propulsion: Gas Turbines and Rockets*, 2nd ed., AIAA Education Series, AIAA, 2006.